Electronic Supplementary Material (ESI) for RSC Advances.


Supporting Information

# A Fast UV-Curable PU-PAAm Hydrogel with Mechanical Flexibility and Self-Adhesion for Wound Healing

Yi Hou[1], Nan Jiang[1], Dan Sun[2, *], Yiping Wang[1], Xianchun Chen[1], Songsong Zhu[1, *], Li Zhang[1, *]

[1] *Analytical & Testing Center, State Key Laboratory of Oral Diseases & National Clinical Research Center for Oral Disease & West China Hospital of Stomatology, School of Materials Science & Engineering, Sichuan University, Chengdu 610065, China*

[2] *Advanced Composite Research Group (ACRG), School of Mechanical and Aerospace Engineering, Queens University Belfast, Belfast BT9 5AH, U.K.*

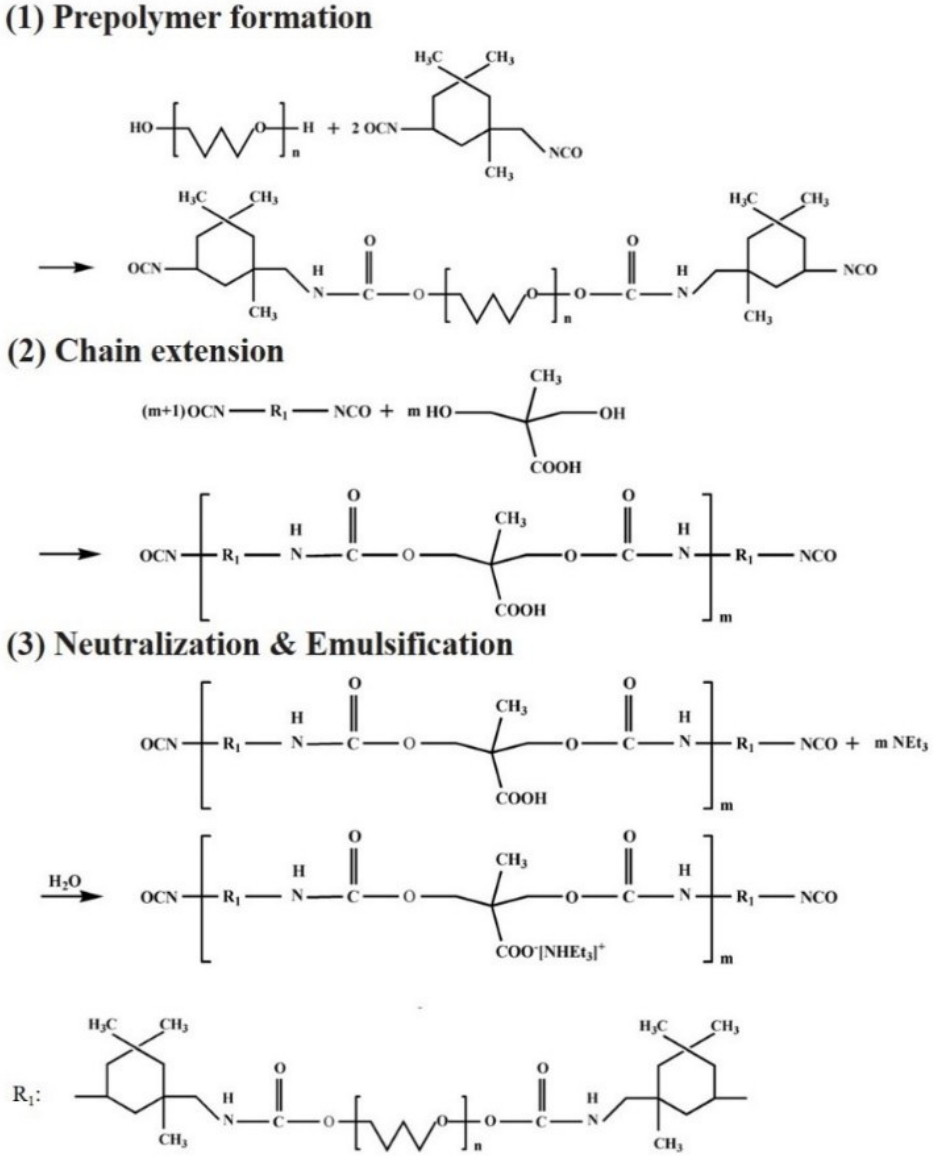


**Figure S1.** Synthetic schemes of PU.

**(1) Free radical production**

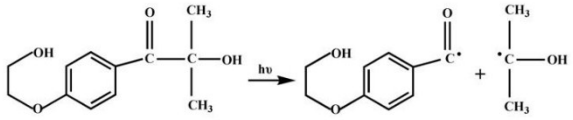

**(2) Chain initiation reaction**

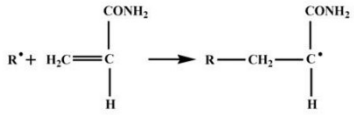

**(3) Chain propagation reaction**

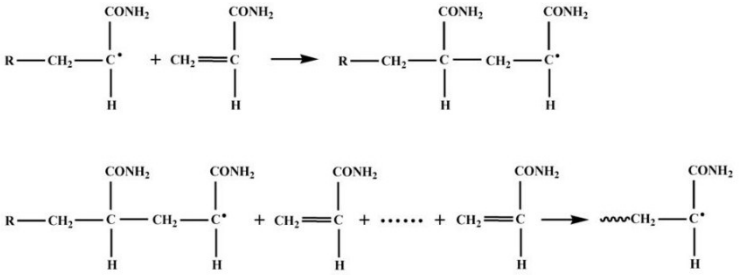

**(4) Crosslinking**

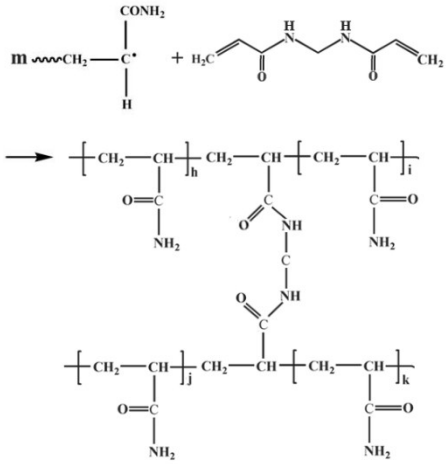

**Figure S2.** Synthetic schemes of PAAm.

**Table S1** Photoinduced PAAm-based hydrogels

| Ref | Chemical composition | Curing conditions | Gelation time | Application |
|---|---|---|---|---|
| [1] | PNIPAAm/PAAm hydrogel | (1) NIPAAm , AAm, (MBAAm) as a cross-linker, $KIO_4$ as a sensitizer;<br>(2) Exposed to the light of a low-pressure Hg lamp (λ = 254-580 nm, 215 W) | **40 min** | Drug delivery system |
| [2] | PAM/poly(DVE-3) hydrogel | (1) AM, DVE-3, EGDMA as a crosslinker, Darocur 1173 as Free radical photoinitiator;<br>(2) Under a high-pressure mercury lamp emitting overwhelmingly light at 365 nm | **1 h** | Sorbent materials in heavy metal removing processes |
| [3] | PAAm based BZ gel | (1) AAm, $[Ru(bpy)_2(4\text{-methyacryloylmethyl-40-methylbpy})]^{2+}(PF6^-)_2$, MBAAm as a crosslinker, Darocure 1173 as photo-initiator;<br>(2) under a mask aligner with a 298 nm UV light source, at 300 watt power (exposure dose = 8mJ $cm^{-2}$) | **60 s** | |
| [4] | P(AAm-co-VDT-co-SPAA) hydrogel | (1) AAm, VDT, SPAA, PEGDA as a crosslinker, PBPO as photoinitiator;<br>(2) under white light (LED lamp, 600 lm in intensity), 20 cm from the mixture | **30 min** | Tissue engineering applications |
| [5] | Agar/PAAm hydrogel | (1) Agar, AAm, MBAA, Irgacure 2959, alginate;<br>(2) under UV light (375 nm) with nitrogen gas | **1 h** | Load-bearing tissue substitutes |
| [6] | ALG -PAAm hydrogel | (1) Alginate, EPS, acrylamide, ammonium persulfate (APS) as photoinitiator, N,N' -methylenebis(acrylamide) (BIS) as crosslinker<br>(2) Under a mercury vapour light source (254 nm, 50 $mW/cm^2$) | **2 h** | Potential for tissue-mimicking phantoms and implantable tissue |
| [7] | κ-carrageenan/PAAm | (1) κ-carrageenan, potassium chloride (KCl), acrylamide (AAm), N,N′-methylenebisacrylamide (MBA) used as a chemical cross-linker, and 2-hydroxy-4′-(2-hydroxyethoxy)-2-methylpropiophenone used as a UV initiator<br>(2) under a UV lamp (a wavelength of 365 nm and an intensity of 8 mW/cm2 ) to carry out the photopolymerization reaction for κ-carrageenan/PAAm DN hydrogel. | **1 h** | Robotics and human motion detection. |
| [8] | κ-car/PAm/GO hydrogel | (1) GO, κ-Car, Am, KCl, MBA, and UV-initiator<br>(2) exposed to the UV light (with a wavelength of λ =365 nm at an intensity of 8 W) | **1h** | |

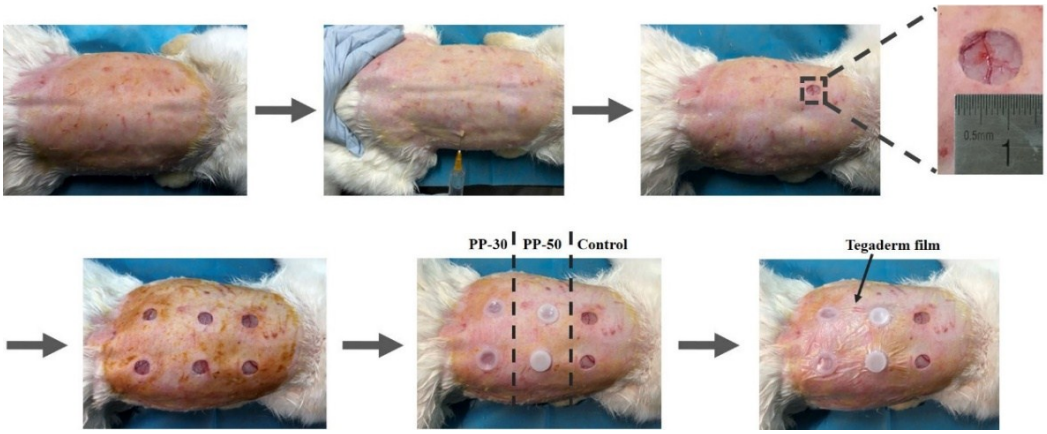


**Figure S3.** The process for creating skin defects and application of PU-PAAm hydrogels.

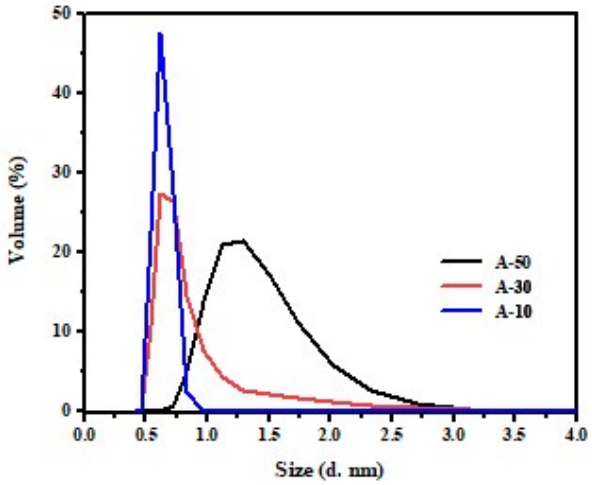


**Figure S4.** Particle-size distribution curves of AAm aqueous solutions (A-50, A-30, A-10 represent AAm solutions with 50% (w/w), 30% (w/w), 10% (w/w) solid contents, respectively).

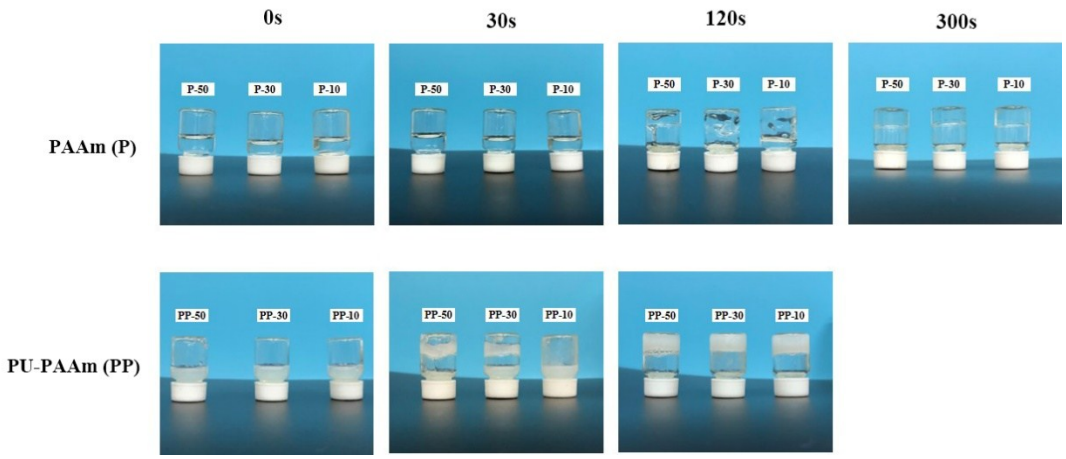


**Figure S5.** Inversion tests of hydrogels with different solid contents under different UV irradiation duration.

SEM images in Figure S6 show that the hydrogels have a highly porous structure with interconnected pores. PU-PAAm hydrogels display larger and more uniform pore size compared with the PAAm hydrogels with the same solid contents. In particular, PP-30 exhibits a looser 3D porous structure due to the incorporation of PU chains and the greater water content.

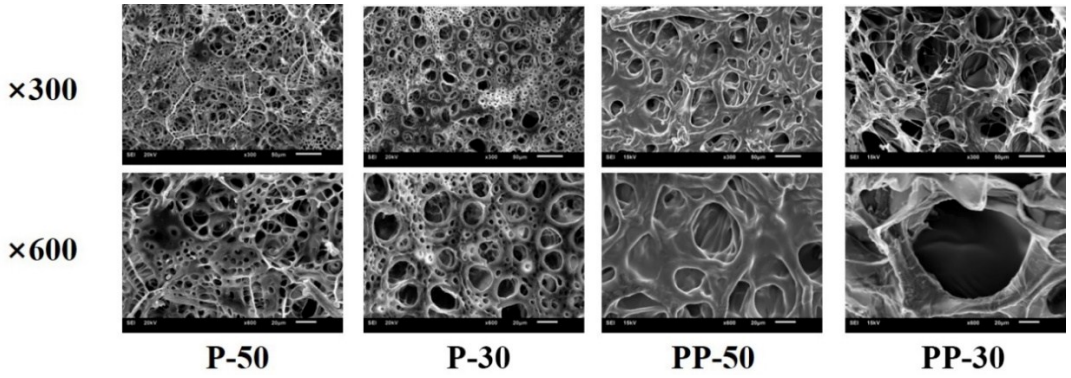


**Figure S6.** SEM images of PAAm and PU-PAAm hydrogels.

DSC and TG curves in Figure S7 exhibit a three-stage weight loss in hydrogels. Stage I weight loss (below 278 °C) was due to the evaporation of free water (about 0-100 ℃) and bound water (100-278 ℃) according to the literature. It can be seen that the weight loss rate of bound water was much slower than that of free water, due to the restraint of hydrogen bonds between water and polymer chains. The stage II weight loss ranging from 278 to 350 ℃ resulted from the decomposition of -CONH groups in PU and the reaction between two amide groups. The stage III weight loss appeared at 350-500 ℃, which could be caused by the disintegration of imides in PAAm and degradation of polyether in soft segments of PU. DSC analysis is also an important way to show the micro-phase segregation and compatibility of PU and PAAm chains. It can be found that the T*g* of P-50, P-30 was 242, 246℃, respectively. The addition of PU shifted the T*g* to lower temperature, compared to that of the PAAm hydrogel with the same solid content, indicating that interpenetrating has occurred between PAAm and PU chains.

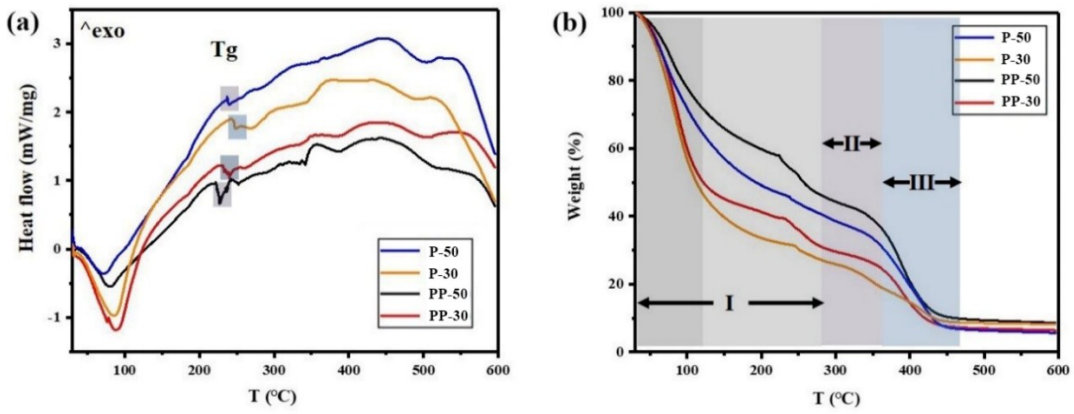


**Figure S7.** DSC (a) and TG (b) curves of of PAAm and PU-PAAm hydrogels.

The inner structure of PAAm-PU hydrogels was further investigated by TEM. As shown in Figure S8, white particles represent PU, while the black region represents PAAm phase. It can be seen that PU uniformly dispersed in the continuous PAAm phase, displaying a typical IPN structure. The phase boundaries of PP-50 and PP-30 are fuzzy and indistinct, suggesting the interpenetration of polymer chains occurred at the PU and PAAm interface. Compared with PP-50, interpenetrated PU particles in PP-30 were more evenly distributed among the continuous phase of PAAm, suggesting that hydrogel with increasing solid content has more tendency for particle agglomeration.

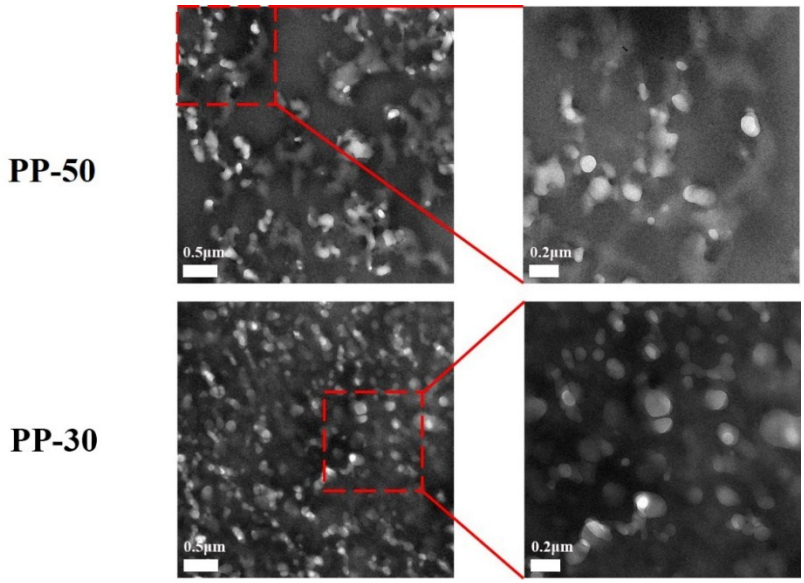


**Figure S8.** TEM images of PAAm and PU-PAAm hydrogels.

SEM images of PAAm and PU-PAAm hydrogels after 28 days swelling test are shown in Figure S9. All hydrogels displayed a highly porous structure with interconnected network. Also, PP-50 and PP-30 displayed larger and more uniform pore size as compared to P-50 and P-30, the trend of which was consistent with the microstructure before swelling.

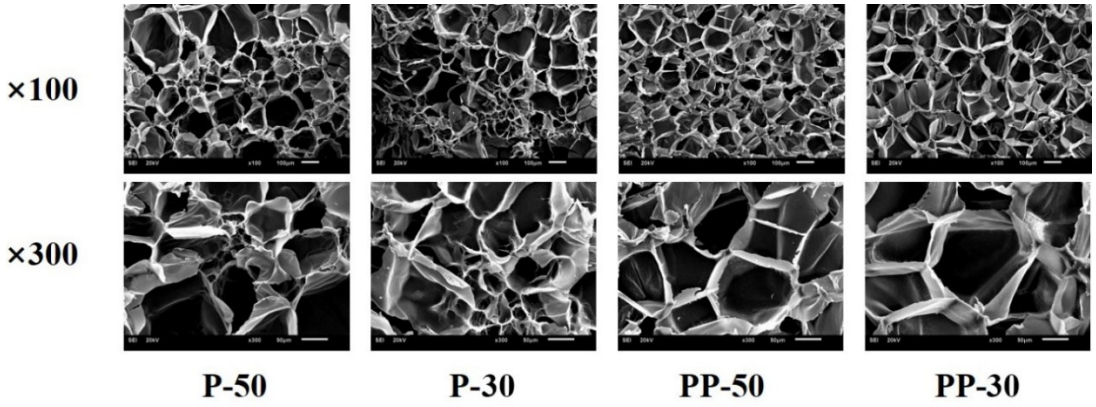


**Figure S9.** SEM images of PAAm and PU-PAAm hydrogels after 28 days of swelling.

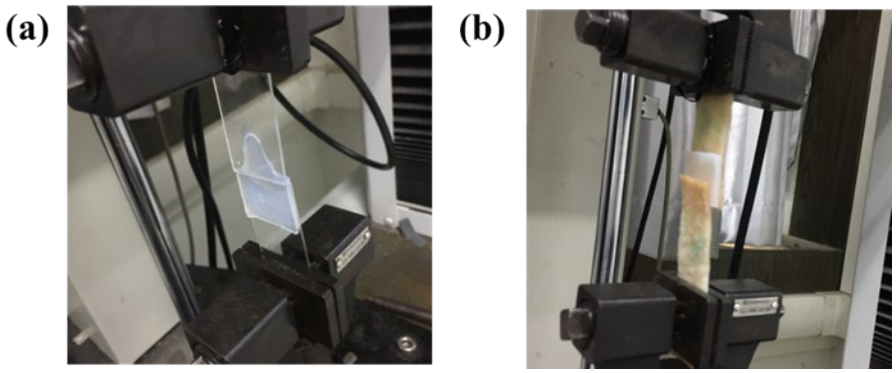


**Figure S10.** Adhesion strength measurement of PU-PAAm adhered to glass slide and porcine skin.

PP-30 was able to endure violent water flushing after adhering to either glass slide or porcine skin.

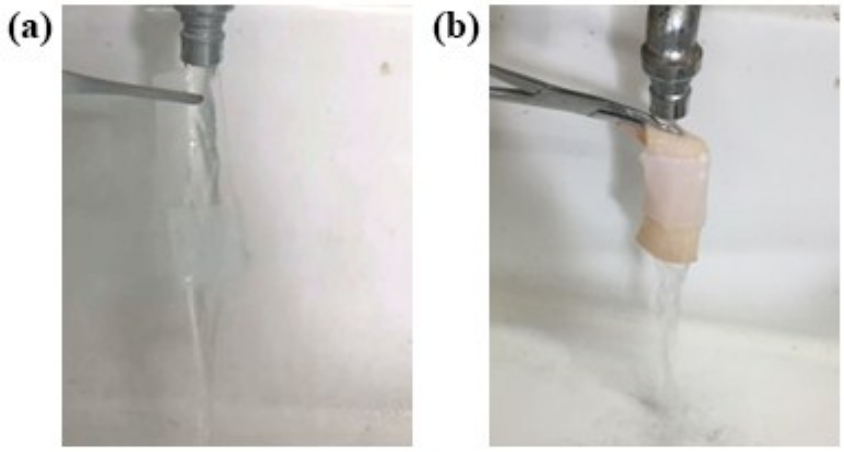


**Figure S11.** Photos of PP-30 adhered to glass slide and porcine skin under vigorous water flushing.

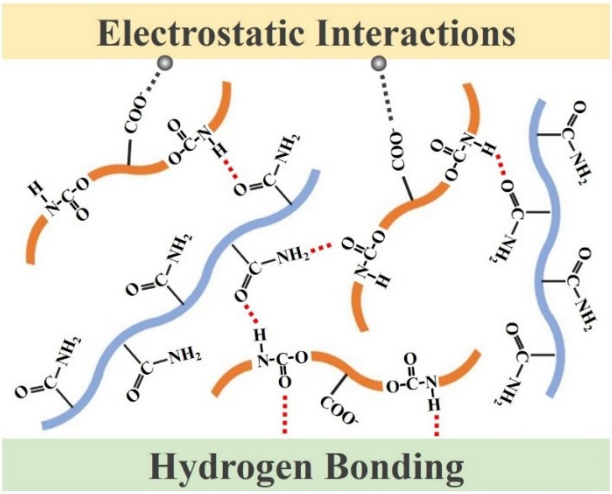


**Figure S12.** Schematic diagram showing interaction mechanism between the hydrogel and the skin.

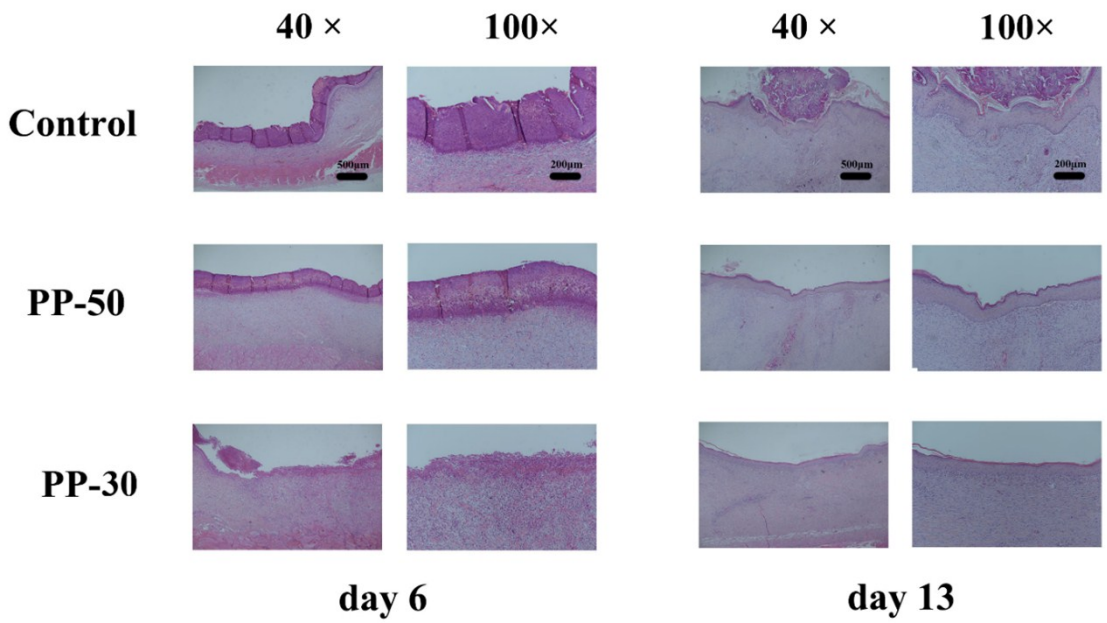


**Figure S13.** Histological evaluation of skin tissues after day 6 and day 13 with HE staining covered by different groups.

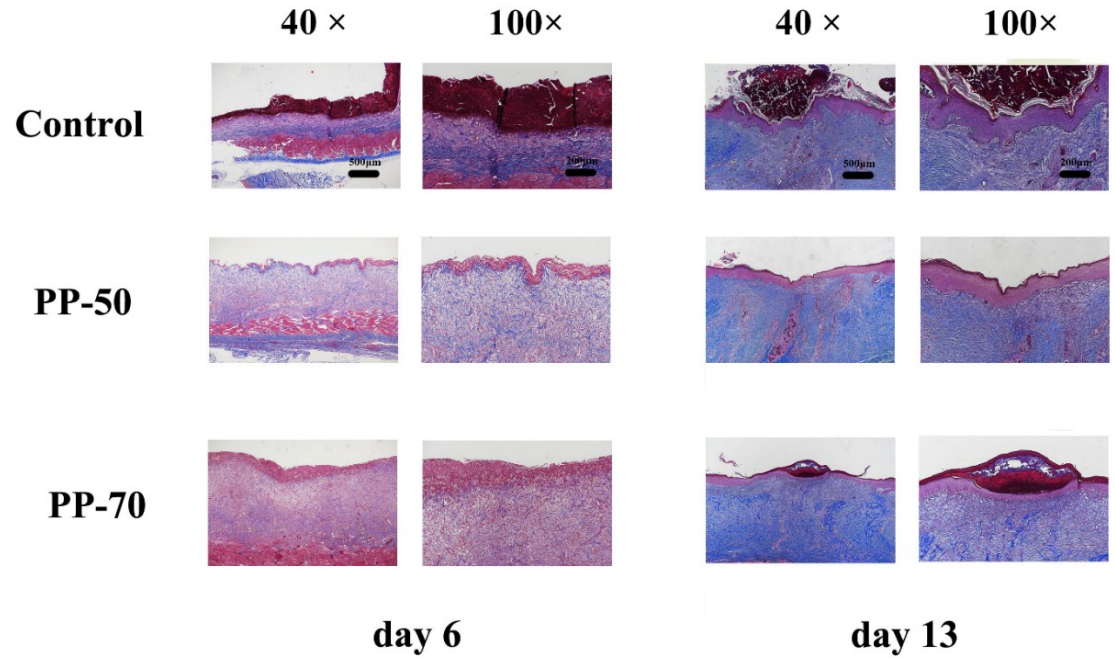


**Figure S14.** Histological evaluation of skin tissues after day 6 and day 13 with Masson staining covered by different groups.

## References


[1] M. R. Guilhermeb, G. M. Campesea, E. Radovanovicb, A. F. Rubirab, E. B. Tambourgia, E. C. Muniz. Thermo-Responsive Sandwiched-Like Membranes of IPN-PNIPAAm/PAAm Hydrogels. *Journal of Membrane Science* **2006**, 275, 187-194.

[2] J. Wang, F. Liu. UV-Radiation Curing of Simultaneous Interpenetrating Polymer Network Hydrogels for Enhanced Heavy Metal Ion Removal. *Materials Science and Engineering B* **2012**, 177, 1633-1640

[3] P. Yuan, O. Kuksenok, D. E. Gross, A. C. Balazs, J. S. Moorea, R. G. Nuzzo. UV Patternable Thin Film Chemistry for Shape and Functionally Versatile Self-Oscillating Gels. *Soft Matter* **2013**, 9, 1231-1243.

[4] N. Wang, Y. Li, Y. Zhang, Y. Liao, W. Liu. High-Strength Photoresponsive Hydrogels Enable Surface-Mediated Gene Delivery and Light-Induced Reversible Cell Adhesion/Detachment. Langmuir **2014**, 30, 11823-11832.

[5] J. Wei, J. Wang, S. Su, S. Wang, J. Qiu, Z. Zhang, G. Christopher, F. Ning, W. Cong. 3D Printing of An Extremely Tough Hydrogel. RSC Adv. **2015**, 5, 81324

[6] Q. Dou, Z. W. K. Low, K. Zhang, X. J. Loh. A New Light Triggered Approach to Develop A Micro Porous Tough Hydrogel. RSC Adv., **2017**, 7, 27449.

[7] S. Liu, L. Li. Ultrastretchable and Self-Healing Double-Network Hydrogel for 3D Printing and Strain Sensor. ACS Appl. Mater. Interfaces **2017**, 9, 26429-26437

[8] S. Tarashia, H. Nazockdasta, G. Sodeifian. A Comparative Study on Microstructure, Physical-Mechanical Properties, and Self-Healing Performance of Two Differently Synthesized Nanocomposite Double Network Hydrogels Based on κ-car/PAm/GO. Polymer **2020**, 188, 122138.